549387

Sandia National Laboratories
Operated for the U.S. Department of Energy by
Sandia Corporation

Albuquerque, New Mexico 87185-

date: 29 July 2008
to: Records
from: A. E. Ismail 7/29/08
M. B. Nemer 7/29/08
Tech: J. W. Garner
QA: M. J. Chavez
Mgmt: M. Y. Lee
subject: Radium-226 Concentrations in the CRA-2009 PA

1. Radium-226 Concentration in Replicate 1, Scenario 1, Vector 53 in the CRA-2009 Performance Assessment

The statutory requirements of 40 CFR 194.55 require that DOE determine the maximum total radioactivity level for radium-226 and radium-228 in any underground source of drinking water (USDW) for 10,000 years after disposal as part of the 2009 Compliance Recertification Application. Radium-226 and radium-228 are obtained as decay products from the following chains:

$$^{238}\text{Pu}$$
$$\downarrow$$
$$^{242}\text{Pu} \rightarrow ^{238}\text{U} \rightarrow {}^{234}\text{U} \rightarrow {}^{230}\text{Th} \rightarrow {}^{226}\text{Ra} \rightarrow {}^{210}\text{Pb}$$
$$^{244}\text{Cm}$$
$$\downarrow$$
$$^{252}\text{Cf} \rightarrow {}^{248}\text{Cm} \rightarrow {}^{244}\text{Pu} \rightarrow {}^{240}\text{Pu} \rightarrow {}^{236}\text{U} \rightarrow {}^{232}\text{Th} \rightarrow {}^{228}\text{Ra}$$

Although the statutory requirements stipulates that the concentrations of both ^{226}Ra and ^{228}Ra be computed, it can be shown that the majority of the radium in the repository occurs as ^{226}Ra, and we can therefore use the concentration of ^{226}Ra to bound the total radium concentration. To justify this claim, we note that, ^{228}Ra has a half-life of 6.7 years and an inventory at closure of 3.94 Ci for both the Compliance Recertification Application 2004 Performance Assessment Baseline Calculation (CRA-2004 PABC) and the CRA-2009 (Garner and Leigh 2005). Since ^{232}Th, the parent of ^{228}Ra, has a half-life of 1.4×10^{10} years, the two species will reach secular equilibrium with 3.42 Ci of ^{228}Ra. However, this is at all times lower than the concentration of ^{226}Ra, which starts at 4.56 Ci and increases to 50 Ci at 10,000 years. Consequently, the concentration of ^{226}Ra at the Land Withdrawal Boundary (LWB) can be used to constrain the total radium concentration.

Previous approaches to determining the concentration of these radium isotopes in drinking water has been to use scoping calculations (U.S. DOE 1996, U.S. DOE 2004) to place an upper bound of the concentration. However, since the inventories of all of the radionuclides are computed using PANEL, it is possible to use the nuclide transport code NUTS to determine the concentration of radium exiting through the LWB, if we assume that the source term for radium is equal to 1 molar.

To carry out these calculations, we therefore modified the standard input file used for NUTS in the CRA-2009 PA to include tracking of ^{226}Ra. Then, after retrieving the needed BRAGFLO and PANEL files from their respective CMS libraries, NUTS was re-run for Vector 53 of Replicate 1, the only vector showing the potential for releases through the marker bed during the screening step of NUTS in the

CRA-2009 PA (Ismail and Garner 2008). Files stored as part of the CRA-2004 PABC or the CRA-2009 PA and retrieved for the present calculations are listed in Table 1. A number of additional files were created for use with these calculations and are stored in the class RADIUM in libraries LIBCRA1BC_NUT and LIBCRA09_NUT, respectively; these files are listed in Table 2. All output files created as a result of these scripts are also found in the indicated classes. The results of MBCON.EXE, a post-processing data extraction program, were verified by visual inspection.

Table 1 PA files used as inputs for the determination of radium-226 concentrations at the LWB

File	Library	CRA-2009 PA	CRA-2004 PABC
BF2_CRA09_R1_S1_V053.INP	LIBCRA09_BFR1S1	X	
BF2_CRA1BC_R1_S1_V053.INP	LIBCRA1BC_BFR1S1		X
BF3_CRA09_R1_S1_V053.CDB	LIBCRA09_BFR1S1	X	
BF3_CRA1BC_R1_S1_V053.CDB	LIBCRA1BC_BFR1S1		X
PANEL_CON_CRA1BC_R1_S1_V053.CDB	LIBCRA1BC_PANEL	X	X
MBCON.FOR (MBCON.EXE)	LIBCRA09_NUT	X	X
NUTS_QA0205C.EXE	LIBCRA09_NUT	X	X

Table 2 Input files and scripts used for the determination of radium-226 concentrations at the LWB

File	Purpose
ISO_CONC.COM	Script to execute codes required for the calculation
PA_NUTS_ISO_S1_CONC.INP	ALGEBRA input file
PA_NUTS_ISO_S1_CONC.SMZ	SUMMARIZE input file

The principal output file for these calculations is PA_NUTS_ISO_S1_CONC.TBL, which lists the concentrations of each of six radionuclides, including ^{226}Ra, as a function of time. The data files—one each for the CRA-2009 PA and the CRA-2004 PABC—were imported into SigmaPlot and used to produce the plot shown in Figure 1.

The maximum concentration of ^{226}Ra, 1.7×10^{-16} Ci/L for the CRA-2009 PA and 6.5×10^{-19} Ci/L for the CRA-2004 PABC, is found for both analyses at 10,000 years. In neither case, however, does the concentration of ^{226}Ra exceed even 5.0×10^{-16} Ci/L, which is nearly four orders of magnitude below the statutory limit of 5 picocuries per liter. The cause of the increase is related to the change in the porosity parameter for intact halite (S_HALITE:POROSITY), which was incorrectly defined in the CRA-2004 PABC (Ismail 2008). To demonstrate that this parameter was responsible for the change in porosity, an additional set of BRAGFLO and NUTS calculations were performed.

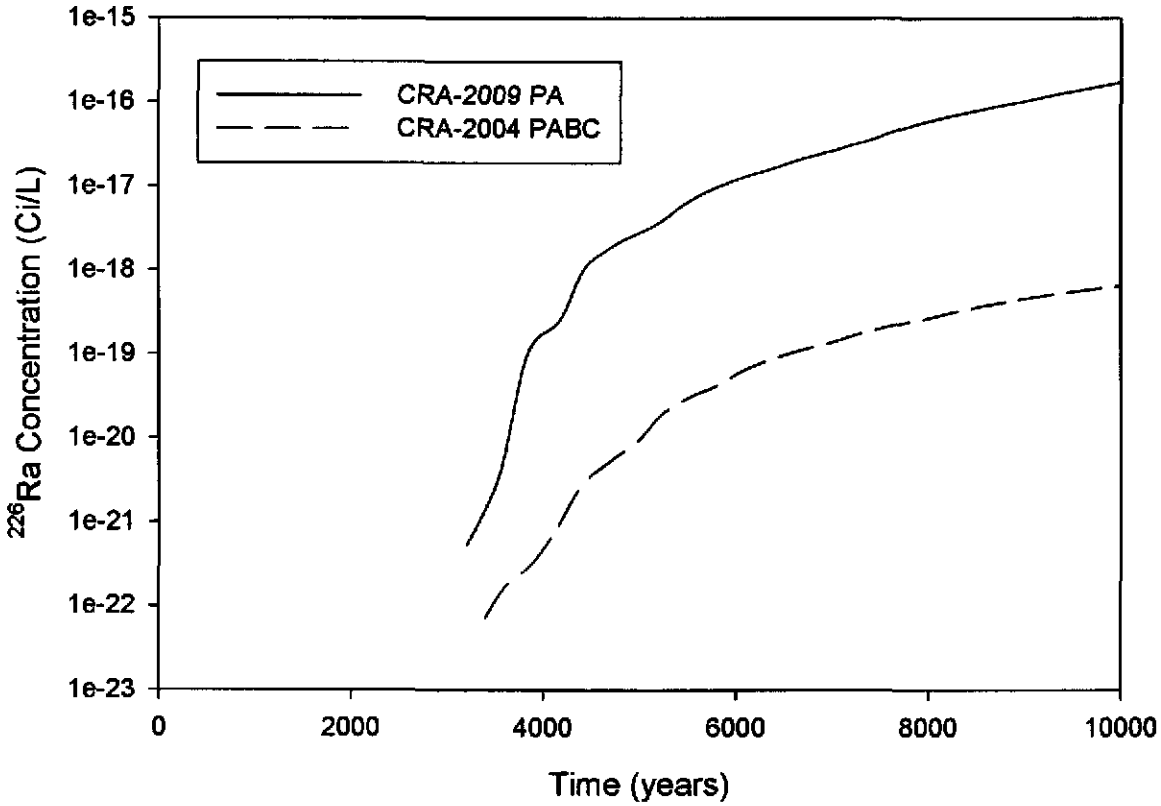

Figure 1 Radium-226 concentration at the LWB as a function of time for Replicate 1, Vector 53 of the CRA-2009 PA and the CRA-2004 PABC

The file BF2_CRA09_R1_S1_V053.INP was modified to produce the input file BF2_CRA09_MPOR_R1_S1_V053.INP by changing the values on lines 1408, 1409, 1426, 1427, 1450 and 1451 by copying lines 1365, 1366, 1383, 1384, 1403 and 1404 of the input file BF2_CRA1BC_R1_S1_V053.INP, respectively. This changed the values of the S_HALITE, DRZ_0, DRZ_1 and DRZ_PCS porosities and fracture model parameters to match those used in the CRA-2004 PABC. These files were then used in BRAGFLO; the output files were passed to NUTS, and used to determine the amount of radium-226 transported across the LWB. The requisite files for this calculation are stored in class OLDPOROS of the CMS library LIBCRA09_NUT.

The concentrations of ^{226}Ra outside the LWB as a function of time for this run, plus the others plotted in Figure 1, are shown in Figure 2. It can be seen that the concentration profiles of the CRA-2009 PA using the CRA-2004 PABC porosity value are essentially the same as the results of the CRA-2004 PABC itself. From this, we can conclude that the change in the porosity distribution is the driver for the increase in radium concentrations observed in the CRA-2009 PA. The increased porosity causes a small increase in fluid flow, which in turn leads to an increase in the distance which brine travels away from the repository. Numerical dispersion effects required by NUTS causes the leading edge of the contaminated brine to advance one cell further, which causes a significantly higher concentration reported at the LWB; we examine the causes of this increase in concentration below.

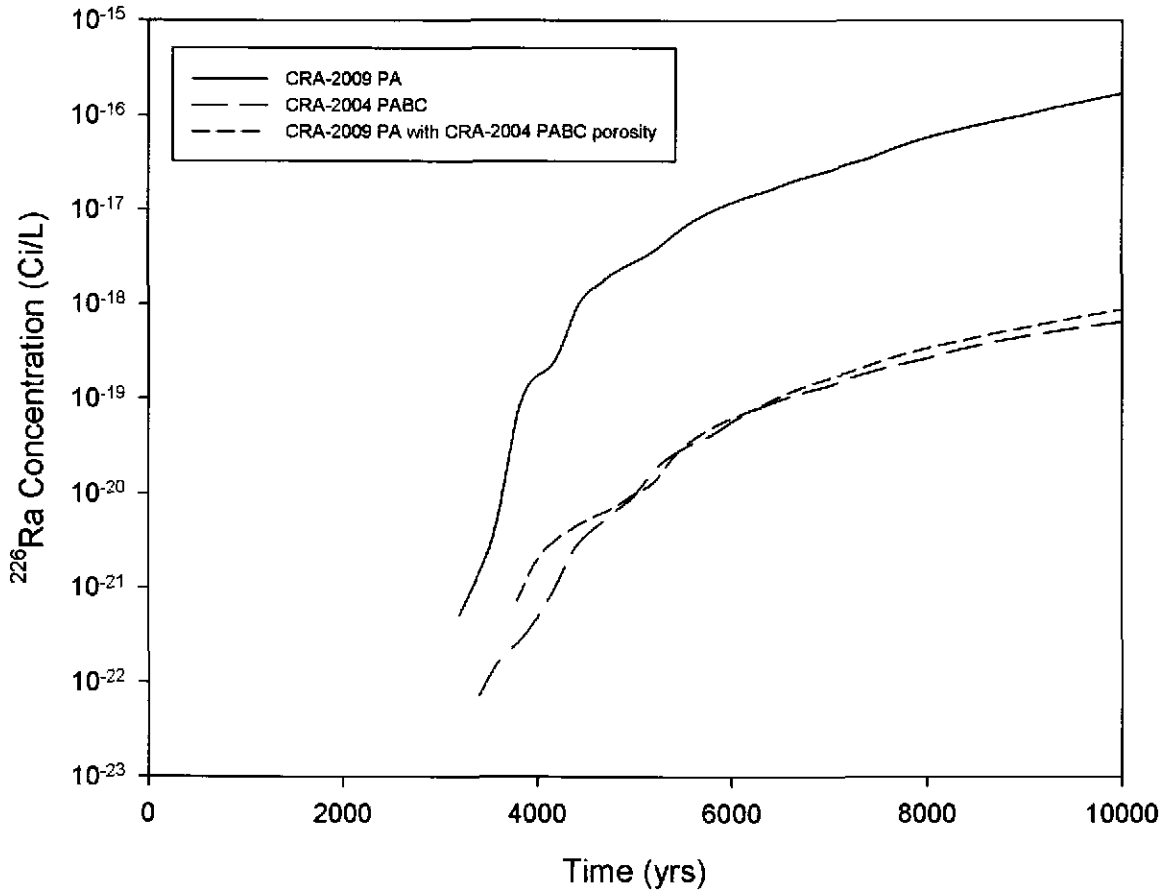

Figure 2 Radium-226 concentration at the LWB as a function of time for Replicate 1, Vector 53 of the CRA-2009 PA and the CRA-2004 PABC, plus the results of using the CRA-2009 PA parameters except for the CRA-2004 PABC porosity value.

2. Numerical Dispersion Effects on Radium-226 Concentrations in the CRA-2009 Performance Assessment

As discussed in the previous section, a several-hundred-fold increase in the concentration of radionuclides reaching the LWB was observed in the CRA-2009 PA calculations compared to that of the CRA-2004 PABC. The large increase occurred only in marker bed 139 south of the repository. Figure 1 shows the Salado flow and transport grid. In this section we explain why this increase is the result of numerical dispersion and is not representative of increased travel distance of the radionuclide front towards the LWB.

The code NUTS (Gilkey, 2006) uses the darcy flow field in the Salado, calculated by BRAGFLO, to obtain estimates of transport times of radionuclides leaving the repository. NUTS assumes no diffusion or dispersion, hence transport occurs by advection only. The advection problem is governed by the well-known wave equation

$$\frac{\partial C}{\partial t} + \frac{u}{\phi}\nabla C = 0, \qquad (1)$$

where C is concentration, t is time, u is the darcy velocity, ϕ is porosity, and the gradient is taken with respect to distance.

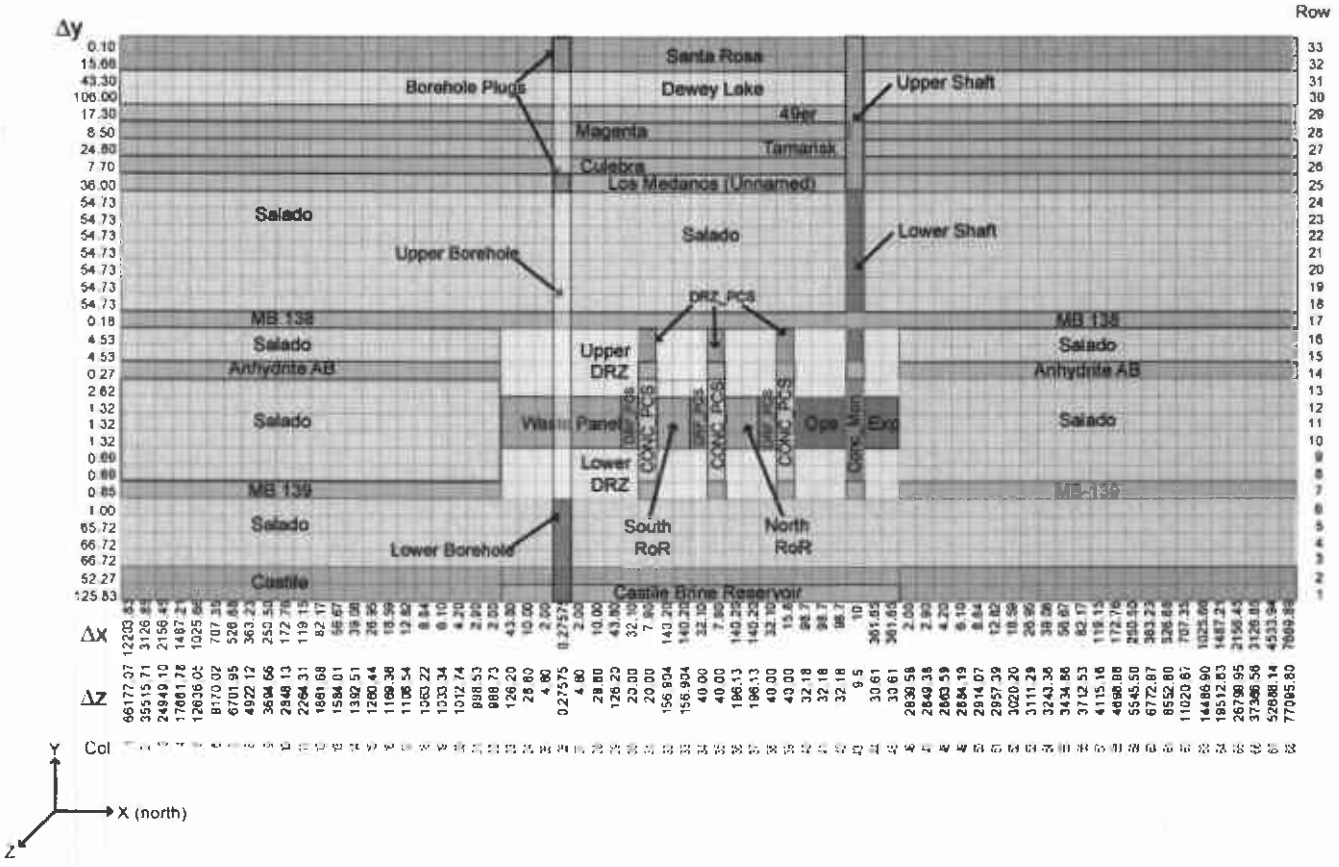

Figure 3 BRAGFLO grid for the CRA-2009 Salado flow and transport calculations. See Nemer and Clayton (2008).

In writing equation (1), we have simplified the problem by approximating porosity as constant in time and space, and approximating the darcy velocity as incompressible,

$$\nabla \cdot \mathbf{u} = 0 . \tag{2}$$

NUTS does not make these approximations but they are useful here for understanding the problem. The solutions to equation (1) are functions of the form $f(x + ut/\phi)$ and $f(x - ut/\phi)$,

$$C = Af\left(x + ut/\phi\right) + Bf\left(x - ut/\phi\right), \tag{3}$$

where x is distance, and A and B are boundary/initial conditions. The wave front in equation (3) propagates linearly with the "mean microscopic velocity" u/ϕ (see Chapter 3 of de Marsily, 1986), without any alteration of the shape of the front. Thus the function $f(x)$ is the initial wave front at $t = 0$. In the Salado flow and transport grid, it is assumed that at $t = 0$, the radionuclide concentration is zero everywhere except in the waste-filled areas where it is given a finite value. Although this front has a step-function profile ($f(x = 0, t = 0) = 1, f(x > 0, t = 0) = 0$), because NUTS is a finite-difference code and must numerically differentiate and integrate equation (1), the code constructs a first-order continuous ($C^{(1)}$) function of concentration throughout the entire Salado grid. This means that in marker bed 139, the concentration of radionuclides in the grid has a smooth numerical "tail" with distance that proceeds ahead of the actual front, as illustrated in Figure 2. This behavior is a classic example of numerical dispersion. Figure 2 is plotted in semi-log scale and thus the linear behavior

for $x \gg 1$ signifies exponential decay (e^{-ax}) of concentration with distance. This exponential tail is numerical dispersion; it has no physical significance.

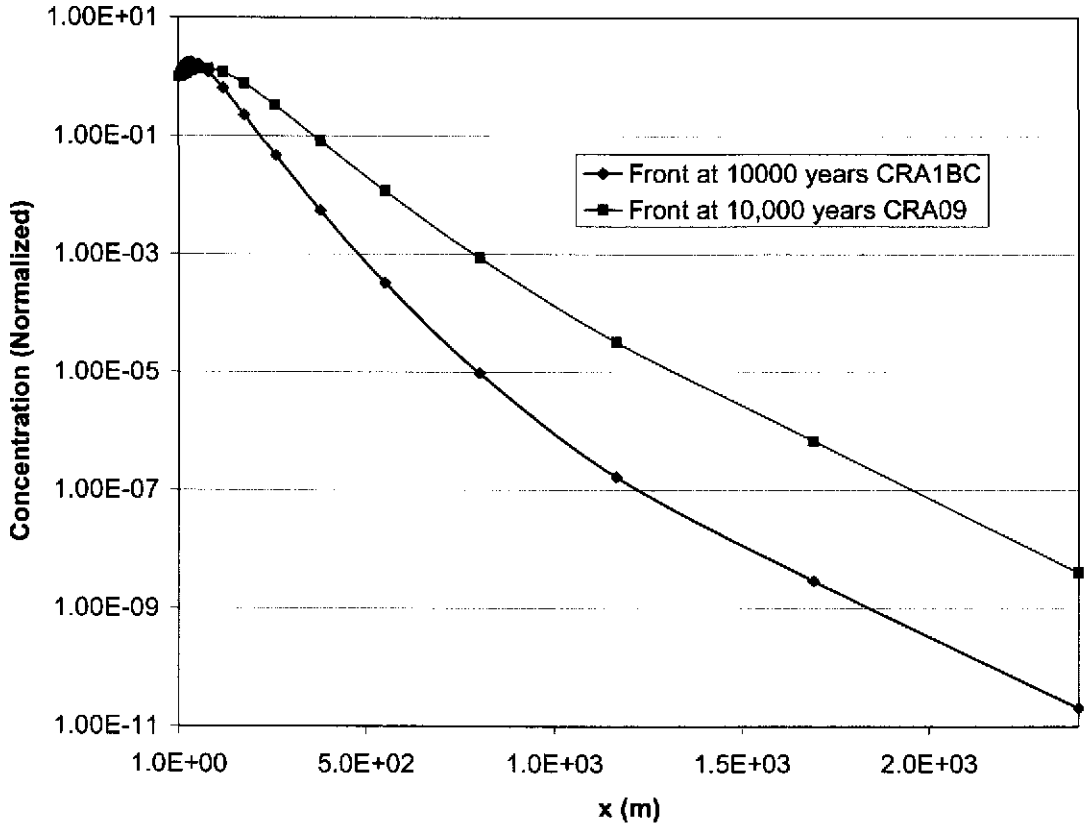

Figure 4 Concentration profile in marker bed 139 normalized by the concentration at the marker bed cell adjoining the waste area (i.e. C(x = 0) = 1) at 10,000 years plotted versus distance (meters) out to the LWB, shown for the CRA-2004 PABC and the CRA-2009 PA. Each symbol corresponds to the southern edge of a grid cell in marker bed 139, see Figure 1. Notice that the actual front has only propagated a few hundred meters while the numerical tail extends to the LWB. This data was obtained from the variable CM1139S in the NUTS screening run files NUT_SCN_CRA1BC_R1_S1_V053.CDB and NUT_SCN_CRA09_R1_S1_V053.CDB, which are located on the PA cluster in LIBCRA1BC_NUTR1S1, class CRA1BC-0 LIBCRA09_NUTR1S1, class CRA09-0, respectively.

To determine a conservative upper bound for how far the front propagates in 10,000 years without numerical dispersion, one can use the darcy velocity maximized over the entire marker bed, u_{max}, at each time and integrate forward in time,

$$x_{max} = \int_{t=0}^{t=10{,}000\ y} \left(\frac{u_{max}(t)}{\phi} \right) dt \,. \tag{4}$$

In order to output darcy velocity in the horizontal direction, it was necessary to rerun BRAGFLO for vector 53 of replicate 1, adding the element variable VELDBRX to the binary output file. This was performed under run control for vector 53 for both the CRA-2004 PABC and the CRA-2009 PA. Table 3 contains the run control information for these runs.

Table 3 Run control information for re-run of vector 53, scenario S1, replicate R1, from the CRA-2004 PABC and CRA-2009 PA.

Analysis*	BRAGFLO Version	POSTBRAG Version	File Name	Library
CRA-2004 PABC	5.0	4.00	BF3_CRA09_R1_S1_V053.CDB	LIBCRA1BC_BFR1S1
CRA-2009 PA	6.0	4.00A	BF3_CRA1BC_R1_S1_V053.CDB	LIBCRA09_BFR1S1

*For both vectors the CDB file is stored in the class RADIUM. All files are stored on the WIPP PA cluster.

Table 4 Front-propagation distances calculated from u_{max} along MB139.

Analysis	Travel Distance at 10,000 years (m)
CRA-2004 PABC	157
CRA-2009 PA	320

From equation (4), we find x_{max} as listed below in Table 4; as can be seen, without numerical dispersion the front has propagated only a short distance away from the repository.

From Figure 4 we can see that the numerical tails for the CRA-2004 PABC and the CRA-2009 PA are roughly parallel. However the CRA-2009 PA tail is shifted forward by about one grid cell. Each symbol in Figure 4 corresponds to the southern edge of a grid cell in marker bed 139, shown in **Figure 3**. Given that the CRA-2009 PA tail propagated one cell further than the CRA-2004 PABC tail and that the tails have an exponential decay with distance, it is not surprising to see a large increase in the tracer concentration at the LWB. While the shift of one grid cell caused a considerable change in concentration, we believe that the grid is still sufficiently well spatially refined because the actual front has not propagated to the cells close to the LWB, and if it had the front would not exhibit such a strong spatial decay. Thus the concentrations obtained at the LWB from NUTS for this vector are only numerical dispersion.

REFERENCES

de Marsily, G. 1986. *Quantitative Hydrogeology.* Academic Press: San Diego.

Garner, J., and Leigh, C. 2005. *Analysis Package for PANEL: CRA-2004 PA Baseline Calculation.* Carlsbad, NM: Sandia National Laboratories. ERMS 540572.

Gilkey, A. P. 2006. "NUTS, Version 2.05C." Carlsbad, NM: Sandia National Laboratories. ERMS 543406.

Ismail, A. E. and Garner, J. W. 2008. Analysis Package for Salado Transport Calculations, Compliance Recertification Application 2009. Carlsbad, NM: Sandia National Laboratories. ERMS 548845.

Nemer, M. and D. J. Clayton. 2008. "Analysis Package for Salado Flow Modeling: 2009 Compliance Recertification Application Calculation." Carlsbad, NM: Sandia National Laboratories. ERMS

U.S. DOE. 1996. Title 40 CFR Part 191 Compliance Certification Application for the Waste Isolation Pilot. DOE/CAO-1996-2184. Carlsbad, NM: U.S. Department of Energy, Carlsbad Field Office.

U.S. DOE. 2004. Title 40 CFR Part 191 Compliance Recertification Application for the Waste Isolation Pilot. DOE/WIPP 2004-3231. Carlsbad, NM: U.S. Department of Energy, Carlsbad Field Office.